

M.A. AL-JUBBORI,<sup>1</sup> H.H. KASSIM,<sup>2</sup> E.M. RAHEEM,<sup>3</sup> I.M. AHMED,<sup>1</sup> Z.T. KHODAIR,<sup>3</sup> F.I. SHARRAD,<sup>4,5</sup> I. HOSSAIN<sup>6</sup>

<sup>1</sup> Department of Physics, College of Education for Pure Science, University of Mosul  
(41001 Mosul, Iraq; e-mail: mushtaq\_phy8@yahoo.com)

<sup>2</sup> Department of Physics, College of Science, University of Kerbala  
(56001 Karbala, Iraq)

<sup>3</sup> Ministry of Science and Technology, Directorate of Nuclear Researches and Applications  
(Baghdad, Iraq)

<sup>4</sup> Department of Physics, College of Science, University of Diyala  
(Diyala, Iraq)

<sup>5</sup> College of Health and Medical Technology, Al-Ayen University  
(64001 Al Nasiriya, Thi-Qar, Iraq; e-mail: fadhil.altiae@gmail.com )

<sup>6</sup> Department of Physics, Rabigh college of Science & Arts, King Abdulaziz University  
(21911 Rabigh, Saudi Arabia)

## NUCLEAR STRUCTURE OF RARE-EARTH $^{172}\text{Er}$ , $^{174}\text{Yb}$ , $^{176}\text{Hf}$ , $^{178}\text{W}$ , $^{180}\text{Os}$ NUCLEI

UDC 539

Using the method with new empiric equation (NEE) and the model of interacting bosons (IBM-1), we study the ground-state band and the gamma- and beta-emission spectra of erbium (Er) and osmium (Os) elements with  $N = 104$ . The absolute  $B(E2)$  strengths for the nuclei are determined. The properties of the potential energy surface are investigated within IBM-1. The ratio  $E\gamma(I+2)/(I)$  as a function of the angular momentum ( $I$ ) and the characteristics of the yrast states are found. The constructed plots indicate that all nuclei of  $^{172}\text{Er}$ ,  $^{174}\text{Yb}$ ,  $^{176}\text{Hf}$ ,  $^{178}\text{W}$ , and  $^{180}\text{Os}$  have a rotational SU(3) character. The staggering factors of available measured data are considered. The results of both models agree well with available experimental data for  $^{172}\text{Er}$ ,  $^{174}\text{Yb}$ ,  $^{176}\text{Hf}$ ,  $^{178}\text{W}$ , and  $^{180}\text{Os}$  nuclei.

*Keywords:* erbium-osmium, ground-state band, NEE, IBM-1,  $B(E2)$ , SU(3).

### 1. Introduction

The study of the neutron-rich deformed nuclei are exciting topics of theoretical and experimental studies. The rare-earth isotopes are of significant interest for nuclear scientists since they exist far away from the spherical form and present an amusing arena for challenging theories of nuclei. These isotopes from lighter to heavier ones involve a rapid change from spherical to non-spherical nuclei. The combined excitation dynamics of non-spherical nuclei significantly depends on nucleons exterior to the occupied shell. The neutron-proton communication plays a main role in damages not disturbing a normal or regular contour of the nucleus.

The combined excitations of a nucleus with even atomic number ( $Z$ ) and even mass ( $A$ ) are pro-

nounced by the number of bosons. Here,  $s$  and  $d$  denote two classes of bosons, where  $s$  and  $d$  correspond, respectively, to  $L^\pi = 0^+$  and  $L^\pi = 2^+$  [1]. There are three regularities of the U(6) assembly: anharmonic vibrator related to U(5),  $\gamma$ -unstable nuclei characterized by O(6), and a deformed rotor with SU(3)[2]. Moreover, there are three additional phenomenological studies: U(5)-SU(3), U(5)-O(6), and SU(3)-O(6) limits [3–5]. Actually, a lot of research articles were carried out with the use of hypothetical and applied comments for the construction of the exceptional earth nuclei [6–17]. In the recent time, the nuclear structures of unusual nuclei of Er, Yb, Hf, W, and Os with the numbers of neutrons equal to 100 and 102 were clarified [18, 19]. These results will give the opportunity to study the deformation for  $N = 104$  of erbium and osmium elements. Moreover, neutron-rich nuclei are particularly interesting, since they might reveal a nuclear structure associated with the access of neutrons.

© M.A. AL-JUBBORI, H.H. KASSIM, E.M. RAHEEM,  
I.M. AHMED, Z.T. KHODAIR, F.I. SHARRAD,  
I. HOSSAIN, 2022

The aim of this paper is to understand the ground-state, gamma-, and beta-bands and a deformation of the E2 strength for Er, Yb, Hf, W, and Os chains with  $N = 104$  by IBM-1 and the technique known as a new empirical equation (NEE). Within IBM-1, the potential energy surfaces (EPSs) for  $^{172}\text{Er}$ ,  $^{174}\text{Yb}$ ,  $^{176}\text{Hf}$ ,  $^{178}\text{W}$ , and  $^{180}\text{Os}$  nuclei are also of interest for finding the dynamical symmetry SU(3) characters.

## 2. Theoretical Method

The Hamiltonian of IBM-1 contains 9 terms [1, 20–24]:

$$\begin{aligned} H = & \varepsilon_s(s^\dagger \tilde{s}) + \varepsilon_d(d^\dagger \tilde{d}) + \sum_{L=0,2,4} \frac{1}{2}(2L+1)^{(1)} \times \\ & \times C_L \left[ [d^\dagger \times d^\dagger] \times [\tilde{d} \times \tilde{d}] \right]^{(0)} + \frac{1}{\sqrt{2}} \nu_2 \left[ [d^\dagger \times d^\dagger]^{(2)} \times [\tilde{d} \times \tilde{s}]^{(2)} + \right. \\ & + [d^\dagger \times s^\dagger]^{(2)} \times [\tilde{d} \times \tilde{d}]^{(2)} \left. \right]^{(0)} + \frac{1}{2} \nu_o \left[ [d^\dagger \times d^\dagger]^{(0)} \times [\tilde{s} \times \tilde{s}]^{(0)} + \right. \\ & + [s^\dagger \times s^\dagger]^{(0)} \times [\tilde{d} \times \tilde{d}]^{(0)} \left. \right]^{(0)} + \frac{1}{2} u_o \left[ [s^\dagger \times s^\dagger]^{(0)} \times [\tilde{s} \times \tilde{s}]^{(0)} + \right. \\ & \left. + u_2 \left[ [d^\dagger \times s^\dagger]^{(2)} \times [\tilde{d} \times \tilde{s}]^{(2)} \right]^{(0)} \right]. \end{aligned} \quad (1)$$

The  $N_b$  (pairs) are conserved,  $N_b = N_s + N_d$  [22]. The Hamiltonian [22, 23]

$$\hat{H} = \varepsilon \hat{n}_d + a_o \hat{P} \hat{P} + a_1 \hat{L} \hat{L} + a_2 \hat{Q} \hat{Q} + a_3 \hat{T}_3 \hat{T}_3 + a_4 \hat{P}_4 \hat{T}_4 \quad (2)$$

$\varepsilon$  is the boson energy, and the operators are:

$$\left. \begin{aligned} \hat{n}_d &= (d^\dagger \tilde{d}), \\ \hat{P} &= \frac{1}{2}[(\tilde{d} \tilde{d}) - (\tilde{s} \tilde{s})], \\ \hat{L} &= \sqrt{10}[d^\dagger \times \tilde{d}]^{(1)}, \\ \hat{Q} &= [d^\dagger \times \tilde{s} + s^\dagger \times \tilde{d}] + \chi [d^\dagger \times \tilde{d}]^{(2)}, \\ \hat{T}_r &= [d^\dagger \times \tilde{d}]^{(r)}. \end{aligned} \right\} \quad (3)$$

The definitions of  $\hat{n}_d$ ,  $\hat{P}$ ,  $\hat{L}$ ,  $\hat{Q}$ ,  $\chi$ , and  $\hat{T}_r$  are presented in [21]. The IBM has three dynamic symmetries [22–24]  $\varepsilon$  is the boson energy, and the operators are:

$$\left. \begin{aligned} \text{U(6)} &\supset \text{U(5)} \supset \text{O(5)} \\ \text{SU(3)} \\ \text{O(6)} &\supset \text{O(5)} \end{aligned} \right\} \supset \text{O(2)}. \quad (4)$$

We know that, chain (I) has the U(5) limit,  $\varepsilon$ , chain (II) has the SU(3) limit,  $a_2$  and chain (III),  $\gamma$ -unstable nuclei, have the O(6) limit, as well as  $a_o$  [1, 23, 25]. For three symmetries, the eigenvalues are [22]:

$$\left. \begin{aligned} E &= \varepsilon n_d + \beta n_d(n_d + 4) + \\ &+ 2\gamma\nu(\nu + 3) + 2\delta L(L + 1) \dots \text{U(5)}, \\ E &= \frac{a_2}{2}(\lambda^2 + \mu^2 + \lambda\mu + 3(\lambda + \mu) + \\ &+ (a_1 - \frac{3a_2}{8})L(L + 1) \dots \text{SU(3)}, \\ E &= \frac{a_o}{4}(N - \sigma)(N + \sigma + 4) + \\ &+ \frac{a_3}{2}\tau(\tau + 3) + \left(a_1 - \frac{a_3}{10}\right)L(L + 1) \dots \text{O(6)}, \end{aligned} \right\} \quad (5)$$

$\gamma$ ,  $\beta$ , and  $\delta$  are the the parameters [26]. Seeing the measured records of  $^{172}\text{Er}$ ,  $^{174}\text{Yb}$ ,  $^{176}\text{Hf}$ ,  $^{178}\text{W}$ ,  $^{180}\text{Os}$  nuclei, we have updated a NEE for GSB [18]:

$$E(I) = \frac{A_1 I(I+1)}{A_2(I+1) + IA_3}, \quad (6)$$

$A_1$ ,  $A_2$  and  $A_3$  were predicted by the measured energies of GSB. The  $\gamma$ - and  $\beta$ -bands are calculated [18] as:

$$E(I) = E_o + \frac{(A_1 + B)(I(I+1))}{A_2(I+1) + IA_3}. \quad (7)$$

## 3. Results and Discussion

The results of calculations of the ground-state band (GSB), gamma- and beta- bands, and the values of reduced transition probabilities  $B(E2)$  in the framework of IBM-1 and NEE are discussed as follows: The nuclei of the unusual-earth elements  $^{172}\text{Er}$ ,  $^{174}\text{Yb}$ ,  $^{176}\text{Hf}$ ,  $^{178}\text{W}$ , and  $^{180}\text{Os}$  have  $Z = 68, 70, 72, 74$ , and 76, respectively. We have considered the rare-earth  $^{172}\text{Er}$ ,  $^{174}\text{Yb}$ ,  $^{176}\text{Hf}$ ,  $^{178}\text{W}$ ,  $^{180}\text{Os}$  isotones with the number of neutrons  $N = 104$ . These nuclei exist near to those with double magic nucleons  $^{208}\text{Pb}$ . The numbers of protons and neutrons of these nuclei near to the mid shell are described by the SU(3) group. These nuclei have the boson number  $N_b$  from 18 to 14.

The ratio  $R = (E4_1^+)/E2_1^+$  has been calculated to find the primary information about the anharmonic vibrator with U(5) symmetry,  $\gamma$ -unstable nuclei with O(6), and deformed rotor with SU(3). We recall the values  $R = 2.0$  for U(5), 2.5 for O(6), and 3.33 for SU(3) [1, 26–28]. Table 1 which display the

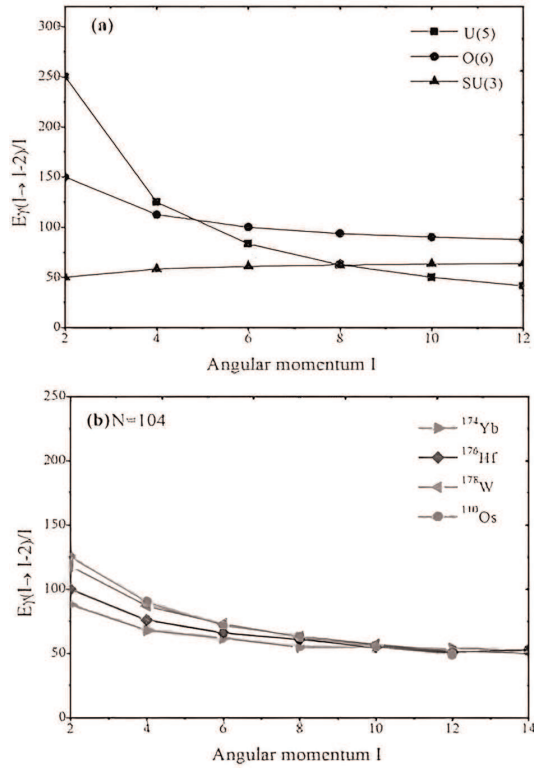


**Fig. 1.** The  $E\gamma(I \rightarrow I - 2)/I$  versus the angular momentum  $I$  for three limits of a vibrator possessing  $U(5)$ ,  $\gamma$ -soft one with  $O(6)$ , and a rotator with  $SU(3)$  (a). E-GOS curves of  $^{172}\text{Er}$ ,  $^{174}\text{Yb}$ ,  $^{176}\text{Hf}$ ,  $^{178}\text{W}$ ,  $^{180}\text{Os}$  nuclei for  $N = 104$  (b)

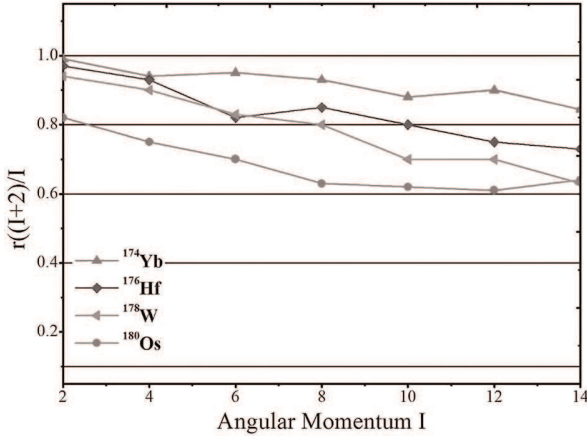


**Fig. 2.** (The factor  $r((I+2)/I)$  versus  $I$  for rare-earth  $^{172}\text{Er}$ ,  $^{174}\text{Yb}$ ,  $^{176}\text{Hf}$ ,  $^{178}\text{W}$ ,  $^{180}\text{Os}$  nuclei

ratios of measured values  $R = E_{4_1}^+ / E_{2_1}^+$  of  $^{172}\text{Er}$ ,  $^{174}\text{Yb}$ ,  $^{176}\text{Hf}$ ,  $^{178}\text{W}$ , and  $^{180}\text{Os}$  isotones. The value  $R4/2 = 3.33$  of those nuclei is related to  $SU(3)$ . For

the three limits, we have [29–31]:

$$\left. \begin{aligned} \text{Vibrational: } R &= \frac{\hbar}{I} \text{ when } I \rightarrow \infty, \\ \text{Rotational: } R &= \frac{\hbar^2}{2\theta} \left( 4 - \frac{2}{I} \right) \rightarrow 4 \frac{\hbar^2}{2\theta} \text{ when } I \rightarrow \infty, \\ \gamma - \text{soft: } R &= \frac{E_{2_1}^+}{4} \left( 1 + \frac{2}{I} \right) \rightarrow \frac{E_{2_1}^+}{4} \text{ when } I \rightarrow \infty. \end{aligned} \right\} \quad (8)$$

Figure 1, a displays  $E\gamma(I \rightarrow 2)/I$  versus the angular momentum  $I$  for three theoretical limits. The  $^{172}\text{Er}$ ,  $^{174}\text{Yb}$ ,  $^{176}\text{Hf}$ ,  $^{178}\text{W}$ , and  $^{180}\text{Os}$  isotones with  $N = 104$  for the E-GOS curvatures are shown in Fig. 1, b. These nuclei are well deformed. The symmetry is calculated to be [38–44]:

$$r \left( \frac{(I+2)}{I} \right) = \left[ R \left( \frac{(I+2)}{I} \right)_{\text{exp}} - \frac{(I+2)}{I} \right] \times \frac{I(I+1)}{2(I+2)}. \quad (9)$$

Here,  $R((I+2)/I)_{\text{exp}}$  is the term corresponding to the levels  $(I+2)$  and  $I$ . Actually the values  $r = 0$  for  $U(5)$ ,  $r = 1$  for  $SU(3)$ , and  $r$  have midway standards for  $O(6)$ . In Eq. (9), the  $r$  factors are improved by 0.10 and 1.0 [39, 41]:

$$\begin{aligned} 0.10 &\leq r \leq 0.35 \text{ for } U(5), \\ 0.40 &\leq r \leq 0.60 \text{ for transitional nuclei}, \\ 0.60 &\leq r \leq 1.0 \text{ for } SU(3). \end{aligned} \quad (10)$$

Figure 2 shows the value of  $r((I+2)/I)$  vs  $I$  for the GSB of  $^{172}\text{Er}$ ,  $^{174}\text{Yb}$ ,  $^{176}\text{Hf}$ ,  $^{178}\text{W}$ , and  $^{180}\text{Os}$  nuclei. The energies of GSB,  $\gamma$ -, and  $\beta$ -bands and  $B(E_2)$  standards for these elements with  $N = 104$  have been considered within the NEE method with software MATLAB 7.0 and IBM with PHINT code [43]. The parameters used in calculations are given in Tables 2 and 3.

The relations among the three factors of the NEE are exposed in Fig. 3 for GSB. The  $A_1$  shows the same

**Table 1. The  $R4/2$  [32–37] for selected nuclei**

Isotopes	Neutron number $N = 104$				
	$^{172}\text{Er}$	$^{174}\text{Yb}$	$^{176}\text{Hf}$	$^{178}\text{W}$	$^{180}\text{Os}$
$R4/2$	3.314	3.309	3.284	3.236	3.093

value for  $^{172}\text{Er}$  and  $^{174}\text{Yb}$  nuclei, and they significantly increase from  $^{176}\text{Hf}$  to  $^{180}\text{Os}$  nuclei. The parameters  $A_2$  and  $A_3$  have no effect on the calculation, and they are overlap with each other for all selected nuclei.

Figure 4 displays the level scheme of the yrast band calculated by IBM-1 and NEE and the measured statistics [32–37] for selected nuclei. The calculated yrast bands of these nuclei are well agree with the measured ones. The excitation heights in a GSB increase unceasingly with aggregate  $Z$  for all even-even selected isotopes with  $N = 104$ . In addition, the factor  $R4/2$  is equal to 3.093 in  $^{180}\text{Os}$  which is not accompanied with SU(3) or U(5).

The calculations of the  $\beta$  and  $\gamma$  bands for all studied nuclei are performed by IBM-1 and NEE, and the comparison with measured data is presented in Tables 4 and 5, respectively. It is shown that both models are in agreement with experiments. The levels with “\*” for the spin-parity are not confirms yet.

The odd-even staggering  $\Delta E_{1,\gamma}(I)$  ( $\Delta I = 1$  staggering) in the gamma bands has been found by the

**Table 2. Parameters of IBM-1 and NEE in MeV, excluding  $N$ ,  $A_2$  and  $A_3$  for  $^{172}\text{Er}$ – $^{180}\text{Os}$**

Isotops	$N_b$	IBM			NEE		
		EPS	ELL	QQ	$A_1$	$A_2$	$A_3$
$^{172}\text{Er}$	18	–	0.016	-0.019	12.314	0.014	-0.075
$^{174}\text{Yb}$	17	–	0.014	-0.030	12.435	0.013	-0.042
$^{176}\text{Hf}$	16	–	0.020	-0.024	15.800	0.025	-0.048
$^{178}\text{W}$	15	–	0.027	-0.022	20.500	0.047	-0.048
$^{180}\text{Os}$	14	–	0.037	-0.017	24.500	0.060	-0.060

**Table 3. Parameters of NEE of beta- and gamma- bands in MeV for selected isotones**

Isotops	$N_b$	IBM		NEE	
		$E_0$	$B$	$E_0$	$B$
$^{172}\text{Er}$	18	1.3220	-8.6680	0.8841	0.59967
$^{174}\text{Yb}$	17	1.4878	-1.3931	1.5631	-0.47131
$^{176}\text{Hf}$	16	1.1415	-3.4950	1.2488	0.6719
$^{178}\text{W}$	15	0.9261	-1.8607	1.0610	-2.6282
$^{180}\text{Os}$	14	0.7293	-4.3435	0.6024	9.6322

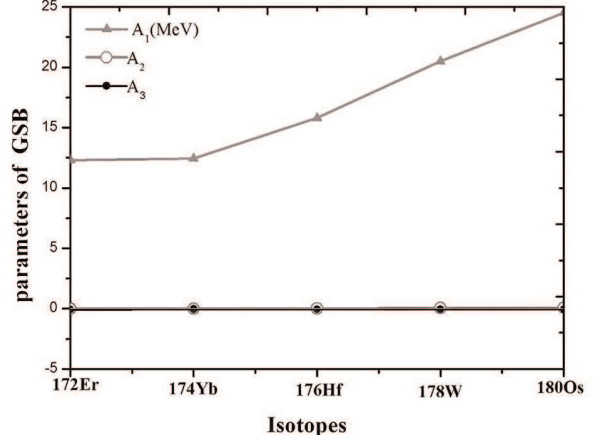


**Fig. 3.** The  $A_1$ ,  $A_2$ , and  $A_3$  parameters of NEE in GSB of all nuclei

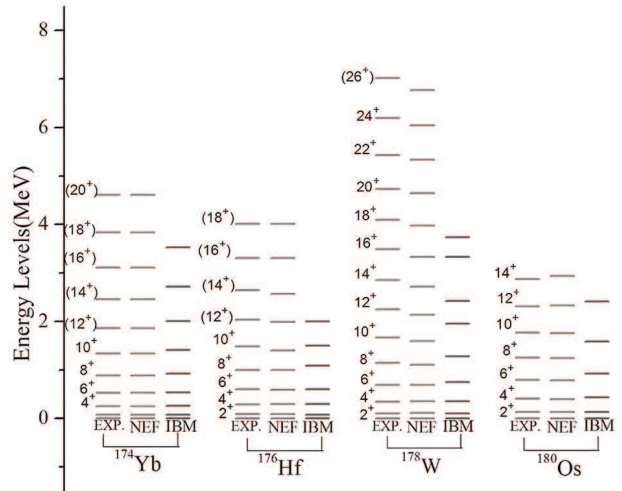


**Fig. 4.** Yrast level of experiments [32–37], NEE, IBM-1 of Er–Os isotopes for  $N = 104$

expression [40–42, 44, 45]:

$$\Delta E_{1,\gamma}(I) = \frac{1}{16} [6E_{1,\gamma}(I) - 4E_{1,\gamma}(I-1) - 4E_{1,\gamma}(I+1) + E_{1,\gamma}(I-2) + E_{1,\gamma}(I+2)], \quad (11)$$

$$E_{1,\gamma}(I) = E_{1,\gamma}(I+1) + E(I). \quad (12)$$

The staggering results are shown in Figs. 5, 6, 7, 8, and 9 for even  $^{172}\text{Er}$ ,  $^{174}\text{Yb}$ ,  $^{176}\text{Hf}$ ,  $^{178}\text{W}$ ,  $^{180}\text{Os}$ , respectively. The  $B(E_2)$  strength can be obtained using the  $T^{E_2}$  operator as [22, 47, 48]:

$$B((E_2)I_i \rightarrow I_f) = \frac{1}{2L_i + 1} |\langle I_f | T^{(E_2)} | I_i \rangle|^2, \quad (13)$$

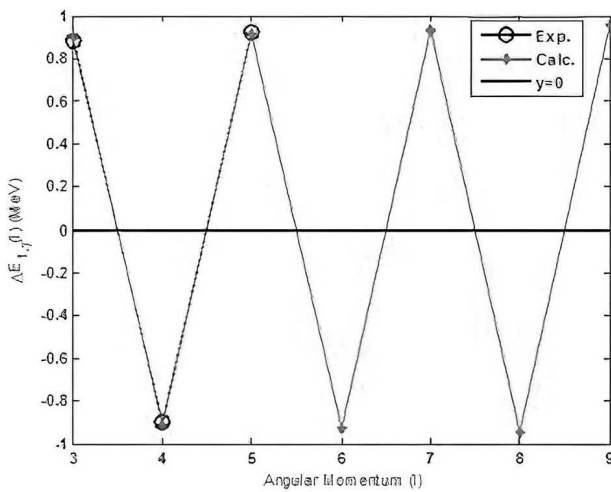


Fig. 5. Staggering of  $^{172}\text{Er}$  isotopes [32–33]

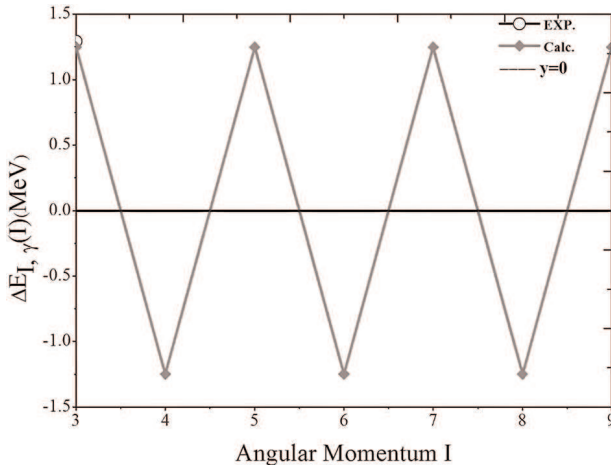


Fig. 6. Staggering of  $^{174}\text{Yb}$  isotope [32–34]

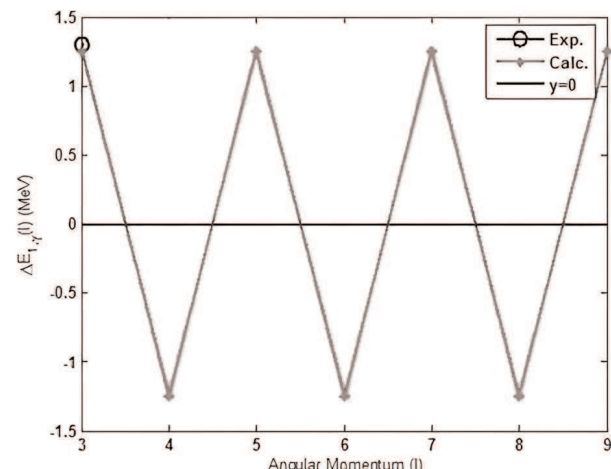


Fig. 7. Staggering of  $^{176}\text{Hf}$  isotope [32–34]

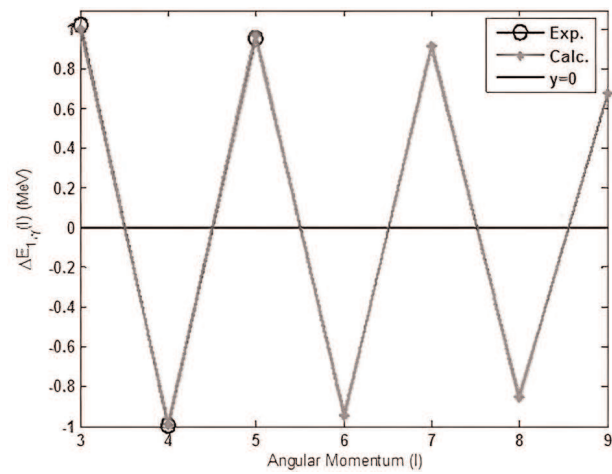


Fig. 8. Staggering of  $^{178}\text{W}$  isotope [32–34, 36]

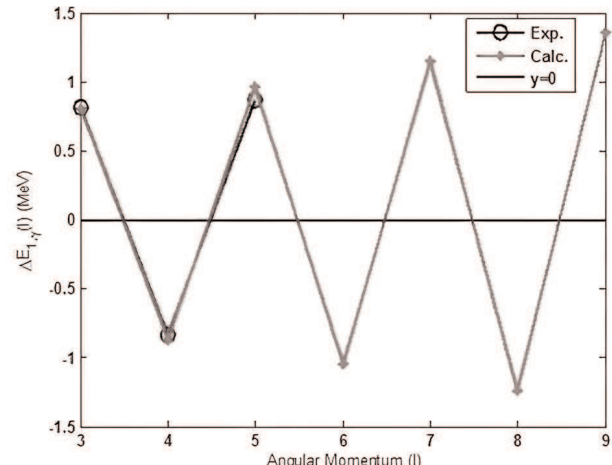


Fig. 9. Staggering of  $^{180}\text{Os}$  isotope [32–37]

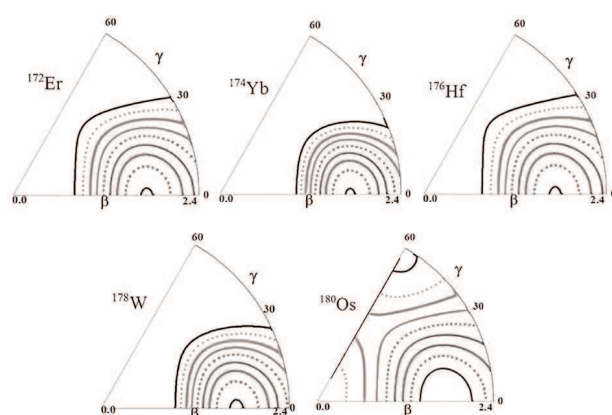


Fig. 10. (Color online) the potential energy surfaces for even-even Er–Os nuclei

$$T^{E_2} = e_B \hat{Q}, \quad (14)$$

where  $e_B$  is the effective charge of a boson, and  $\hat{Q}$  is the quadrupole operator. The values of  $\alpha_2$  and  $\beta_2$  are given in Table 6. The details of calculations of  $\alpha_2$  and  $\beta_2$  are presented in [18,19]. The experimental and calculated data (IBM and NEE) on  $B(E_2)$  strengths are given in Table 7 for selected Er–Os isotopic. The electrical transitions are described by the formula [49]

$$B(E_2) = \frac{0.05657}{T_{1/2}^\gamma(\text{ps}) E_\gamma^5(\text{MeV})} (e^2 b^2), \quad (15)$$

$$T_{1/2}^\gamma = T_{1/2}(\exp)(1 + \alpha_{\text{tot}}). \quad (16)$$

$T_{1/2}$  is a half-life, and  $\alpha_{\text{tot}}$  is the total internal conversion coefficient. Table 7 indicates that, for the rare-earth (Er–Os) selected nuclei, the  $B(E_2)$  strengths

Table 4.  $\beta$ -band (in MeV)  
of  $^{172}\text{Er}$ – $^{180}\text{Os}$  nuclei for  $N = 104$

$I^\pi$	$^{172}\text{Er}$			$I^\pi$	$^{174}\text{Yb}$		
	Exp.	NEE	IBM		Exp.	NEE	IBM
0+	1.322	1.322	1.275	0+	1.487	1.487	1.478
2+	–	1.344	1.352	2+	1.561*	1.554	1.505
4+	1.396*	1.396	1.531	4+	1.701	1.396	1.685
6+	–	1.479	1.814	6+	1.959*	1.955	1.969
8+	–	1.588	2.200	8+	–	–	2.358
10+	–	1.722	2.485	10+	–	–	2.852
12+	–	1.880	–	12+	–	–	3.454
$I^\pi$	$^{176}\text{Hf}$			$I^\pi$	$^{178}\text{W}$		
	Exp.	NEE	IBM		Exp.	NEE	IBM
0+	1.149	1.141	1.141	0+	0.997	0.926	0.981
2+	1.226	1.212	1.229	2+	1.082	1.0274	1.056
4+	1.333	1.373	1.442	4+	1.275	1.244	1.305
6+	1.628	1.614	1.776	6+	1.556	1.554	1.696
8+	1.932*	1.925	2.232	8+	1.915	1.936	2.230
10+	2.294*	2.298	2.811	10+	2.339	2.377	2.709
12+	–	–	3.512	12+	2.804	2.866	3.326
$I^\pi$	$^{180}\text{Os}$			$I^\pi$	$^{180}\text{Os}$		
	Exp.	NEE	IBM		Exp.	NEE	IBM
0+	0.736	0.729	0.636	2+	0.870	0.782	0.851
2+	0.831	0.835	0.776	3+	1.022	0.950	0.991
4+	1.052	1.059	1.103	4+	1.196	1.161	1.177
6+	1.376	1.371	1.617	5+	1.405	1.410	1.409

from  $\beta \rightarrow g$  and  $\gamma \rightarrow g$  transitions are smaller than those for the transitions  $g \rightarrow g$ ,  $\beta \rightarrow \beta$ ,  $\gamma \rightarrow \gamma$  and  $\gamma \rightarrow \beta$ . The calculated data on  $B(E_2)$  in both

Table 5.  $\gamma$ -band (in MeV)  
of selected Er–Os [32–37] isotones for  $Z = 104$

$I^\pi$	$^{172}\text{Er}$			$I^\pi$	$^{174}\text{Yb}$		
	Exp.	NEE	IBM		Exp.	NEE	IBM
2+	0.961*	0.962	1.082	2+	1.634*	1.637	1.756
3+	1.034*	1.042	1.157	3+	1.709*	1.713	1.582
4+	1.131*	1.149	1.257	4+	1.716*	1.815	1.743
5+	1.251*	1.282	1.382	5+	1.926*	1.940	1.814
6+	1.500*	1.440	1.532	6+	2.572*	2.089	2.150
7+	1.654*	1.622	1.707	7+	–	2.260	2.236
8+	1.828*	1.827	1.907	8+	–	2.453	2.592
9+	2.022*	2.054	2.133	9+	–	2.667	2.667
10+	–	2.303	2.385	10+	–	2.901	3.139
11+	–	2.573	2.662	11+	–	3.154	3.150
12+	–	2.862	2.966	12+	–	3.425	3.775
$I^\pi$	$^{176}\text{Hf}$			$I^\pi$	$^{178}\text{W}$		
	Exp.	NEE	IBM		Exp.	NEE	IBM
2+	1.341	1.339	1.234	2+	1.110	1.1578	1.088
3+	1.445	1.429	1.320	3+	1.236	1.2497	1.163
4+	1.540*	1.546	1.450	4+	1.380	1.3663	1.338
5+	1.727*	1.689	1.572	5+	1.572	1.5050	1.483
6+	1.862*	1.856	1.856	6+	1.669	1.6631	1.731
7+	1.926*	2.045	1.957	7+	1.835	1.8387	1.945
8+	2.112*	2.485	2.309	8+	2.023	2.0299	2.268
9+	2.318*	2.485	2.461	9+	2.226*	2.2351	2.551
10+	2.540*	2.733	2.883	10+	2.444	2.4529	2.949
11+	1.341	2.999	3.084	11+	–	2.6820	3.299
12+	–	3.281	3.315	12+	–	2.9214	–
$I^\pi$	$^{180}\text{Os}$			$I^\pi$	$^{180}\text{Os}$		
	Exp.	NEE	IBM		Exp.	NEE	IBM
2+	0.870	0.782	0.851	2+	0.870	0.782	0.851
3+	1.022	0.950	0.991	3+	1.022	0.950	0.991
4+	1.196	1.161	1.177	4+	1.196	1.161	1.177
5+	1.405	1.410	1.409	5+	1.405	1.410	1.409
6+	1.627	1.690	1.689	6+	1.627	1.690	1.689
7+	1.881	1.997	2.013	7+	1.881	1.997	2.013
8+	–	2.329	2.386	8+	–	2.329	2.386
9+	2.410	2.683	2.802	9+	2.410	2.683	2.802
10+	–	3.054	3.270	10+	–	3.054	3.270

Table 6.  $\alpha_2$   $\beta_2$  parameters (in eb) to produce  $B(E_2)$ 

Isotope	$N_b$	$\alpha$	$\beta$
$^{172}\text{Er}$	18	0.0910	-0.2691
$^{174}\text{Yb}$	17	0.0976	-0.2820
$^{176}\text{Hf}$	16	0.0980	-0.2898
$^{178}\text{W}$	15	0.0900	-0.2662
$^{180}\text{Os}$	14	0.0990	-0.2930

Table 7. The values of  $B(E_2)$  (in  $e^2 b^2$ )

$I_i \rightarrow I_f$	$^{172}\text{Er}$		
	Exp.	NEE	IBM
$2_1^+ \rightarrow 0_1^+$	—	—	1.129
$4_1^+ \rightarrow 2_1^+$	—	—	1.600
$6_1^+ \rightarrow 4_1^+$	—	—	1.736
$8_1^+ \rightarrow 6_1^+$	—	—	1.778
$10_1^+ \rightarrow 8_1^+$	—	—	1.7773
$12_1^+ \rightarrow 10_1^+$	—	—	1.737
$14_1^+ \rightarrow 12_1^+$	—	—	1.677
$16_1^+ \rightarrow 14_1^+$	—	—	1.594
$I_i \rightarrow I_f$	$^{174}\text{Yb}$		
	Exp.	NEE	IBM
$2_1^+ \rightarrow 0_1^+$	1.159	1.289	1.156
$0_2^+ \rightarrow 2_1^+$	0.0077	0.0079	0.000
$2_2^+ \rightarrow 2_1^+$	0.0074	—	0.0002
$4_2^+ \rightarrow 3_1^+$	—	—	1.283
$5_1^+ \rightarrow 3_1^+$	—	—	0.9034
$5_1^+ \rightarrow 4_2^+$	—	—	0.915
$6_1^+ \rightarrow 4_1^+$	2.134	2.078	1.776
$8_1^+ \rightarrow 6_1^+$	2.238	2.229	1.817
$10_1^+ \rightarrow 8_1^+$	1.932	1.928	1.908
$12_1^+ \rightarrow 10_1^+$	2.129	2.102	1.768
$14_1^+ \rightarrow 12_1^+$	1.884	1.851	1.701
$16_1^+ \rightarrow 14_1^+$	—	—	1.613
$I_i \rightarrow I_f$	$^{176}\text{Hf}$		
	Exp.	NEE	IBM
$2_1^+ \rightarrow 0_1^+$	1.072	0.924	1.068
$2_3^+ \rightarrow 0_1^+$	0.0193	—	0.000
$2_3^+ \rightarrow 2_1^+$	—	—	0.000
$2_2^+ \rightarrow 2_1^+$	—	0.036	0.000
$2_2^+ \rightarrow 2_1^+$	1.576	—	1.512
$4_1^+ \rightarrow 2_2^+$	1.764	—	1.638
$8_1^+ \rightarrow 6_1^+$	<2.134	—	1.672
$10_1^+ \rightarrow 8_1^+$	—	—	1.661

Continuation of the Tabl. 7

$I_i \rightarrow I_f$	$^{178}\text{W}$		
	Exp.	NEE	IBM
$2_1^+ \rightarrow 0_1^+$	—	—	0.800
$4_1^+ \rightarrow 2_1^+$	—	—	1.132
$6_1^+ \rightarrow 4_1^+$	—	—	1.224
$8_1^+ \rightarrow 6_1^+$	—	—	1.246
$10_1^+ \rightarrow 8_1^+$	—	—	1.233
$12_1^+ \rightarrow 10_1^+$	—	—	1.196
$14_1^+ \rightarrow 12_1^+$	—	—	1.139
$16_1^+ \rightarrow 14_1^+$	—	—	1.066
$I_i \rightarrow I_f$	$^{180}\text{Os}$		
	Exp.	NEE	IBM
$2_1^+ \rightarrow 0_1^+$	0.850	0.959	0.826
$4_1^+ \rightarrow 2_1^+$	1.157	1.226	1.167
$6_1^+ \rightarrow 4_1^+$	1.206	1.016	1.259
$8_1^+ \rightarrow 6_1^+$	0.458	0.390	1.279

model are well agree with available measured data for  $^{172}\text{Er}$ ,  $^{174}\text{Yb}$ ,  $^{176}\text{Hf}$ ,  $^{178}\text{W}$ ,  $^{180}\text{Os}$  nuclei [32–37] in the literature.

The details of calculations of the potential energy surface (PES) by the IBM are given as follows [41, 50, 51] [41, 50, 51]:

$$|N, B, \gamma\rangle = 1/\sqrt{N!} (b_c^\dagger)^N |0\rangle, \quad (17)$$

where  $N$  is the boson number,  $|0\rangle$  denotes the boson vacuum, and

$$b_c^\dagger = (1 + \beta^2)^{1/2} \left\{ \beta \left[ \cos \gamma (d_0^\dagger) + \sqrt{1/2} \sin \gamma (d_2^\dagger + d_{-2}^\dagger) \right] \right\}. \quad (18)$$

Here  $\beta \geq 0$  and  $\gamma \leq \pi/3$ . The expression for the PES calculation reads

$$\begin{aligned} E(N, \beta, \gamma) &= \langle N, \beta, \gamma | H | N, \beta, \gamma \rangle / \langle N, \beta, \gamma | N, \beta, \gamma \rangle = \\ &= \frac{N \varepsilon_d \beta^2}{(1 + \beta^2)} + \frac{N(N+1)}{(1 + \beta^2)^2} \times \\ &\times (\alpha_1 \beta^2 + \alpha_2 \beta^3 \cos 3\gamma + \alpha_3 \beta^2 + \alpha_4). \end{aligned} \quad (19)$$

These expressions give (for higher  $N_b$ )  $\beta_{\min} = 1$ ,  $\sqrt{2}$ , and 0 for O(6), SU(3), and U(5), correspondingly. The premeditated potential energy surfaces are exposed in Fig. 10, c for the  $^{172}\text{Er}$ ,  $^{174}\text{Yb}$ ,  $^{176}\text{Hf}$ ,  $^{178}\text{W}$ ,

$^{180}\text{Os}$  isotones with  $N = 104$ . Figure 10 demonstrates that the selected isotopic chain for  $N = 104$  corresponds to the deformed rotational symmetry.

#### 4. Conclusions

The behavior of low-level ground-state, beta-, and gamma-bands and  $B(E2)$  factors have been explored by means of a technique called the new empirical equation (NEE) and the interacting boson model (IBM) for  $^{172}\text{Er}$ ,  $^{174}\text{Yb}$ ,  $^{176}\text{Hf}$ ,  $^{178}\text{W}$ ,  $^{180}\text{Os}$  nuclei. The results by both models were compared to the previous available experimental data and were established to agree with each other. The E-GOS and the factor  $r((I + 2)/I)$  curvatures of the GSB of Er-Os elements for  $N = 104$  were schemed and investigated for the virtual limits of rotational, vibrational, and  $\gamma$ -soft symmetries. Moreover, all selected nuclei have SU(3) symmetry. The staggering bends,  $\Delta E_{1,\gamma}(I)$  playing a role of spin for  $^{172}\text{Er}$ ,  $^{174}\text{Yb}$ ,  $^{176}\text{Hf}$ ,  $^{178}\text{W}$ ,  $^{180}\text{Os}$  chains of isotones do not turn to zero. The contour plots of PES of selected isotones are distorted and show the SU(3) symmetry. The calculations within NEE and IBM models describe unambiguously the selected isotopes and provide a useful information to test the validity of recently developed nuclear theories and explain the behavior of the nuclear deformation.

We thank Department of Physics, College of Science, University of Kerbala, Department of Physics, College of Education for Pure Science, University of Mosul for supporting this work.

1. F. Iachello, A. Arim. *The Interacting Boson Model* (Cambridge University Press, 1987) [ISBN: 9780511895517].
2. F. Iachello. Analytic description of critical point nuclei in a spherical-axially deformed shape phase transition. *Phys. Rev. lett.* **87**, 052502 (2001).
3. F. Iachello. Dynamic symmetries at the critical point. *Phys. Rev. lett.* **85**, 3580 (2000).
4. P. Cejnar, J. Jolie, R.F. Casten. Quantum phase transitions in the shapes of atomic nuclei. *Rev. Mod. Phys.* **82**, 2155 (2010).
5. R.F. Casten, E.A. McCutchan. Quantum phase transitions and structural evolution in nuclei. *J. Phys. G* **34**, R285 (2007).
6. P.E.A. McCutchan, N.V. Zamfir. Simple description of light W, Os, and Pt nuclei in the interacting boson model. *Phys. Rev. C* **71**, 054306 (2005).
7. A. Dewald, O. Möller, B. Saha, et al. Test of the critical point symmetry X(5) in the mass  $A = 180$  region. *J. Phys. G. Nucl. Partic.* **31**, S1427 (2005).
8. Z. Jin-Fu, L. Li-Jun, B. Hong-Bo. Critical behaviour in nuclear structure from spherical to axially symmetric deformed shape in IBM. *Chinese Phys.* **16**, 7 (2007).
9. S.F. Shen, Y.B. Chen, F.R. Xu, S.J. Zheng, B. Tang, T.D. Wen. Signature for rotational to vibrational evolution along the yrast line. *Phys. Rev. C* **75**, 047304 (2007).
10. P.N. Usmanov, A.A. Okhunov, U.S. Salikhbaev, A.I. Vdovin. Analysis of electromagnetic transitions in nuclei  $^{176,178}\text{Hf}$ . *Phys. Part. Nuclei Lett.* **16**, 185 (2010).
11. K. Nomura, T. Otsuka, N. Shimizu, L. Guo. Derivation of IBM Hamiltonian for deformed nuclei. *J. Phys.: Conf. Ser.* **267**, 012050 (2011).
12. H.L. Liu, F.R. Xu, P.M. Walker, C.A. Bertulani. Deformation and its influence on K isomerism in neutron-rich Hf nuclei. *Phys. Rev. C* **83**, 067303 (2011).
13. X. Hao, L.H. Zhu, X.G. Wu, et al. Evolution of the X(5) critical-point symmetry in rotating  $^{176}\text{Os}$ . *J. Phys. G. Nucl. Partic.* **38**, 025102 (2011).
14. A.A. Raduta, P. Buganu. Application of the sextic oscillator with a centrifugal barrier and the spheroidal equation for some X(5) candidate nuclei. *J. Phys. G. Nucl. Partic.* **40**, 025108 (2013).
15. E. Williams, et al. High-precision excited state lifetime measurements in rare earth nuclei using LaBr<sub>3</sub>(Ce) detectors. *EPJ Web of Conferences* **35**, 06006 (2012).
16. A. Okhunov, F.I. Sharrad, A.A. Al-Sammarea, M.U. Khan-daker. Correspondence between phenomenological and IBM-1 models of even isotopes of Yb. *Chinese Phys. C* **39**, 084101 (2015).
17. S.N. Abood, M.A. Al-Jubbori. Nuclear structure and electromagnetic transitions investigation in Er isotopes within framework of interacting boson model. *textit{Commun. Theor. Phys.}* **60**, 335 (2013).
18. M. Abed Al-Jubbori, H.H. Kassim, F.I. Sharrad, I. Hossain. Deformation properties of the even-odd rare-earth Er-Os isotopes for  $N = 100$ . *Int. J. Mod. Phys. E* **27**, 1850035 (2018).
19. M. Abed Al-Jubbori, H.H. Kassim, A.A. Abd-Aljabbar, H.Y. Abdullah, I. Hossain, I.M. Ahmed, F.I. Sharrad. Nuclear structure of the even-odd rare-earth Er-Os nuclei for  $N = 102$ . *Indian. J. Phys.* **94**, 379 (2020).
20. A. Arima, F. Iachello. Interacting boson model of collective nuclear states II. The rotational limit. *Ann. Phys.-New York.* **111**, 201 (1978).
21. F. Iachello, K. Abrahams, K. Allart, A.E. Dieperink. *Nuclear Structure. Pub (Plenum, New York and London) Ed. Abrahams K., Allart K., and Diapering AEL* (1881).
22. R. F. Casten, D. D. Warner. The interacting boson approximation. *Rev. Mod. Phys.* **60**, 389 (1988).
23. F. Iachello. Dynamical supersymmetries in nuclei. *Phys. Rev. Lett.* **44**, 772 (1980).
24. H.H. Kassim, A.A. Mohammed-Ali, M. Abed Al-Jubbori, F.I. Sharrad, A.S. Ahmed, I. Hossain. Critical point of the

- <sup>152</sup>Sm, <sup>154</sup>Gd, and <sup>156</sup>Dy isotopes isotopes. *Phys. Atom. Nuclei.* **82**, 211 (2019).
25. A. Arima, F. Iachello. Interacting boson model of collective states I. The vibrational limit. *Ann. Phys.-New. York* **281**, 2 (2000).
26. R.F. Casten, Roma. Simplicity and complexity in nuclear structure. *R. Reports in Phys.* **57**, 515 (2005).
27. E.A. McCutchan, R.F. Casten. Crossing contours in the interacting boson approximation (IBA) symmetry triangle. *Phys. Rev. C* **74**, 057302 (2006).
28. M.A. Al-Jubbori, F.Sh. Radhi, A.A. Ibrahim, S.A. Abdullah Albakrid, H.H. Kassim, F.I. Sharrad. Determine the <sup>134–140</sup>Nd isotopes identity using IBM and NEF. *Nucl. Phys. A* **971**, 35 (2018).
29. P.H. Regan, et al. Signature for Vibrational to Rotational Evolution Along the Yrast Line. *Phys. Rev. Lett.* **90**, 152502 (2003).
30. G. Scharff-Goldhaber, J. Weneser. System of even-even nuclei. *Phys. Rev.* **98**, 212 (1955).
31. B.R. Mottelson, S.G. Nilsson. *Danske Videnskab. Selskab. Mat-fys Medd.(to be published)* **27**, 16 (1953).
32. <http://www.nndc.bnl.gov/chart/getENSDFDatasets.jsp>.
33. B. Singe. Nuclear Data Sheets for  $A = 199$ . *Nucl. Data Sheets.* **108**, 196 (2007).
34. E. Browne, H. Junde. Nuclear data sheets for  $A = 174$ . *Nucl. Data Sheets.* **87**, 15 (1999).
35. M.S. Basunia. Nuclear Data Sheets for  $A = 176$ . *Nucl. Data Sheets.* **107**, 791 (2006).
36. E. Achterberg, O.A. Capurro, G.V. Marti. Nuclear data sheets for  $A = 178$ . *Nucl. Data Sheets.* **110**, 1473 (2009).
37. S.C. Wu, H. Niu. Nuclear Data Sheets for  $A = 180$ . *Nucl. Data Sheets.* **100**, 483 (2003).
38. D. Bonatsos, L.D. Skouras. Successive energy ratios in medium-and heavy-mass nuclei as indicators of different kinds of collectivity. *Phys. Rev. C* **43**, 952R (1991).
39. A.M. Khalaf, A.M. Ismail. Structure shape evolution in lanthanide and actinide nuclei. *Prog. Phys.* **2**, 98 (2013).
40. I. Mamdouh, M. Al-Jubbori. The rotational-vibrational properties of <sup>178–188</sup>Os isotope. *Indian J. Phys.* **89**, 1085 (2015).
41. M.A. Al-Jubbori, H.H. Kassim, F.I. Sharrad, I. Hossain. Nuclear structure of even <sup>120–136</sup>Ba under the framework of IBM, IVBM and new method (SEF). *Nucl. Phys. A* **955**, 101 (2016).
42. I.M. Ahmed, G.N. Flaiyh, H.H. Kassim, H.Y. Abdullah, I. Hossain, F.I. Sharrad. Microscopic description of the even-even <sup>140–148</sup>Ba isotopes using BM, IBM and IVBM. *Eur. Phys. J. Plus.* **132**, 84 (2017).
43. O. Scholten. Computer code PHINT, KVI (Groningen, 1980).
44. D. Bonatsos. Systematics of odd-even staggering in  $\gamma$ -bands as a test for phenomenological collective models. *Phys. Lett. B* **200**, 1 (1988).
45. D. Bonatsos, et al.  $\Delta I = 1$  staggering in octupole bands of light actinides: “Beat” patterns. *Phys. Rev. C* **62**, 024301 (2000).
46. I.M. Ahmed, M.A. Al-Jubbori, H.H. Kassim, H.Y. Abdullah, F.I. Sharrad. Investigation of even-even <sup>220–230</sup>Th isotopes within the IBM, IVBM and BM *Nucl. Phys. A* **977**, 34 (2018).
47. H.H. Kassim, A.A. Mohammed-Ali, F.I. Sharrad, I. Hosseini, K.S. Jassim. Nuclear structure of even <sup>178–182</sup>Hf Isotopes under the framework of interacting Boson model (IBM-1). *Iran. J. Sci. Technol. A.* **42**, 993 (2018).
48. H.H. Kassim, F.I. Sharrad. Energy levels and electromagnetic transition of <sup>190–196</sup>Pt nuclei. *Int. J. Mod. Phys. E* **23**, 1450070 (2014).
49. S. Raman, C.W. Nestor, JR, P. Tikaneny. Transition probability from the ground to the first-excited  $2^+$  state of even-even nuclides. *Atom. Data. Nucl. Data.* **78**, 1 (2001).
50. A.E.L. Dieperink, O. Scholten, F. Iachello. Classical limit of the interacting-boson model. *Phys. Rev. Lett.* **44**, 1747 (1980).
51. H.H. Kassim, F.I. Sharrad. Negative parity low-spin states of even-odd <sup>187–197</sup>Pt isotopes. *Nucl. Phys. A* **933**, 1 (2015).

Received 17.10.21

М.А. Ель-Джуббори, Х.Ж. Кассім,  
Е.М. Рахім, І.М. Ахмед, З.Т. Ходейр,  
Ф.Т. Шаррад, І.Хоссейн

#### ЯДЕРНА СТРУКТУРА

#### РІДКОЗЕМЕЛЬНИХ ЯДЕР

<sup>172</sup>Er, <sup>174</sup>Yb, <sup>176</sup>Hf, <sup>178</sup>W TA <sup>180</sup>Os

Використовуючи метод з новим емпіричним рівнянням та модель взаємодіючих бозонів (IBM-1), ми вивчаємо основний стан і гамма-та бета-спектри ербія (Er) та осмія (Os) з  $N = 104$ . Розраховано абсолютні B(E2) інтенсивності для цих ядер. В рамках моделі IBM-1 вивчено властивості поверхні потенціальної енергії. Знайдено відношення  $E\gamma(I+2)/(I)$  як функцію кутового моменту ( $I$ ) та параметри іраст станів. Побудовано графіки, які вказують на те, що всі ядра <sup>172</sup>Er, <sup>174</sup>Yb, <sup>176</sup>Hf, <sup>178</sup>W та <sup>180</sup>Os мають ротаційну SU(3) симетрію. Розглянуто причини певного впорядкування наявних експериментальних даних. Результати обох моделей добре узгоджуються з експериментальними даними для ядер <sup>172</sup>Er, <sup>174</sup>Yb, <sup>176</sup>Hf, <sup>178</sup>W та <sup>180</sup>Os.

**Ключові слова:** ербій, осмій, смуга для основного стану, нове емпіричне рівняння (NEE), модель взаємодіючих бозонів (IBM-1), B(E2), SU(3).